



# Fermi National Accelerator Laboratory

FERMILAB-Pub-91/304-A  
October 1991

## Grand Unified Theories, Topological Defects and Ultrahigh-Energy Cosmic Rays

IN 93-CR  
69300  
P. 12

*Pijushpani Bhattacharjee,<sup>1</sup> Christopher T. Hill<sup>2</sup> and David N. Schramm<sup>1,3</sup>*

<sup>1</sup>Astronomy and Astrophysics Center, Enrico Fermi Institute,  
The University of Chicago, 5640 S. Ellis Avenue,  
Chicago, IL 60637.

<sup>2</sup>Department of Theoretical Physics,  
Fermi National Accelerator Laboratory,  
P.O.Box 500, Batavia, IL 60510.

<sup>3</sup>NASA/Fermilab Astrophysics Center,  
Fermi National Accelerator Laboratory,  
P.O.Box 500, Batavia, IL 60510.

### Abstract

The ultrahigh-energy (UHE) proton and neutrino spectra resulting from collapse or annihilations of topological defects surviving from the GUT era are calculated. Irrespective of the specific process under consideration (which determines the overall normalization of the spectrum), the UHE proton spectrum always 'recovers' at  $\sim 1.8 \times 10^{11} \text{ GeV}$  after a *partial* Greisen-Zatsepin-Kuz'min 'cutoff' at  $\sim 5 \times 10^{10} \text{ GeV}$  and continues to a GUT-scale energy with a *universal shape* determined by the physics of hadronic jet fragmentation. Implications of our results are discussed.

PACS numbers: 98.80.Cq, 98.70.Sa, 98.60.Ce

(NASA-CR-189841) GRAND UNIFIED THEORIES,  
TOPOLOGICAL DEFECTS AND ULTRAHIGH-ENERGY  
COSMIC RAYS (Fermi National Accelerator  
Lab.) 12 p

CSSL 03B

N92-18273

Unclass

G3/93 0069300

Topological defects[1], e.g., monopoles, cosmic strings, domain walls, superconducting cosmic strings, etc., and various possible hybrid objects made of these, are likely to have been formed in symmetry-breaking phase transitions in the early universe. Because of their topological stability the defects can survive indefinitely, *until and unless physically destroyed* due to collapse, annihilations or other reasons[2–5]. When topological defects are destroyed the energy trapped in them is released in the form of massive quanta (hereafter generically referred to as X particles) of the various fields (gauge bosons, higgs bosons, superheavy fermions) that ‘constitute’ the defects. The X-particles can then decay into known quarks, gluons, leptons, etc, which ultimately materialize into, among other particles, nucleons, gamma rays and neutrinos with energies up to  $\sim m_X$ , the mass of the X-particles released from the defects. If the defects were originally formed in a phase transition at the GUT-scale  $\sim 10^{16} GeV$ , then we have here a possible natural mechanism of production of ultrahigh-energy (UHE) cosmic ray (CR) particles up to an energy of this order, *without any acceleration mechanism*. Below we give a general calculation of the expected evolved proton as well as neutrino spectra resulting from this kind of processes. We assume a  $\Omega_0 = 1$  “flat” universe and a Hubble constant  $H_0 = 100.h \text{ Km.s}^{-1}.Mpc^{-1}$ , with  $h = 0.75$  throughout.

The rate of release of X-particles due to destruction of topological defects can, in general, be effectively expressed in terms of two fundamental parameters entering in the problem, namely, the mass scale  $m_X$  and the Hubble time  $\sim t$ , in the form (with  $\hbar = c = M_{Pl}\sqrt{G} = k_B = 1$ )

$$\frac{dn_X(t_i)}{dt_i} = \kappa m_X^p t_i^{-4+p}, \quad (1)$$

where  $\kappa$  and  $p$  are dimensionless constants whose values depend on the specific process involving specific kind of topological defect, (the ‘amplitude’  $\kappa$  may, in general, depend on  $p$ ), and  $n_X(t_i)$  denotes the number density of the X-particles released at the time  $t_i$ . For example,  $p = 1$  for a system of collapsing cosmic string loops[4,5] as well as for a system of collapsing monopolonia[2,7], while  $p = 0$  for a system of saturated superconducting cosmic

string loops[3]. We shall see below that the observed UHE CR flux gives an upper limit to the possible value of  $\kappa$  for any given value of  $p$ .

We assume that each  $X$  decays into a quark and a lepton each carrying an energy  $m_x/2$ . The quarks fragment and produce jets of hadrons. We use the following hadronic fragmentation formula[2,3] that is consistent with leading log QCD behavior and reproduces well the particle multiplicity seen in GeV–TeV jets in colliders:

$$\frac{dN_h}{dx} \simeq 0.08 \exp\left(2.6\sqrt{\ln(1/x)}\right) (1-x)^2 \left(x\sqrt{\ln(1/x)}\right)^{-1}. \quad (2)$$

In eq.(2),  $x \equiv E/E_{jet}$ ,  $E$  being the energy of any hadron in the jet, and  $E_{jet} \simeq m_x/2$  is the total energy in the jet, and  $N_h$  is the number of hadrons carrying a fraction  $x$  of the total energy in a jet. It turns out[5] that, in the range  $10^{-10} \leq x \leq 10^{-2}$ , Eq.2 is numerically well approximated by a power-law of the form

$$\frac{dN_h}{dx} \simeq 3.322 x^{-1.324}, \quad 10^{-10} \leq x \leq 10^{-2}, \quad (3)$$

which gives rise to a considerably flatter injection spectrum (see below) than the usually assumed UHE CR injection spectrum having a power-law index  $\sim -2.5$ .

Most of the hadrons in a jet will be pions, but a small fraction ( $\sim 3\%$ ) will be nucleons and antinucleons. For the propagation times and energies of our interest most (but not all) of the neutrons and antineutrons in a jet will  $\beta$ -decay to protons and antiprotons which we shall hereafter collectively refer to as protons. From Eq.1, the injection spectrum,  $\Phi_p(E_i, t_i)$ , for protons, i.e., the number density of protons injected per unit energy interval at an injection energy  $E_i$  per unit time at an injection time  $t_i$ , is (with  $x \equiv 2E_i/m_x$ )

$$\Phi_p(E_i, t_i) = \frac{dn_x}{dt_i}(t_i) \times 0.03 \times \frac{2}{m_x} \frac{dN_h}{dx}.$$

Each charged pion (in the jets) after decay ultimately gives rise to three neutrinos— one  $\nu_\mu$ , one  $\bar{\nu}_\mu$ , and one  $\nu_e$  (or  $\bar{\nu}_e$ )— all of roughly the same energy. The  $\nu_\mu + \bar{\nu}_\mu$  injection spectrum resulting from charged pion decay can be written as[8]

$$\Phi_\nu(E_i, t_i) = 2 \times \frac{dn_x}{dt_i}(t_i) \times 2.343 \times \frac{2}{m_x} \times 0.97 \int_{4.686E_i/m_x}^1 \frac{1}{x} \frac{dN_h}{dx} dx.$$

Note that, except for the overall source evolution factor  $dn_x/dt_i$  given by Eq. 1, the basic form of injection spectrum (for both protons and neutrinos) is determined by the micro-physics of hadronic jet fragmentation and not by any external astrophysical parameters.

For any injection spectrum  $\Phi(E_i, t_i)$  due to a isotropic source distribution, the particle flux (i.e., the number of particles crossing unit area per unit time per unit solid angle per unit energy interval) today, for ultrarelativistic particles traveling along straight-line paths in a  $\Omega_0 = 1$  universe is

$$\begin{aligned} j(E_0) &= \frac{c}{4\pi} \int_{t_{i,min}}^{t_0} dt_i (1+z_i)^{-3} \Phi(E_i, t_i) \left( \frac{dE_i}{dE_0} \right)_{E_0} \\ &= \frac{3}{8\pi} ct_0 \int_0^{z_{i,max}(E_0)} dz_i f(E_i, z_i), \end{aligned}$$

where

$$f(E_i, z_i) = \begin{cases} (1+z_i)^{-5.5} \Phi(E_i, z_i) \left( \frac{dE_i}{dE_0} \right)_{E_0}, & \text{if } z_i \leq z_{eq}, \\ \frac{4}{3} \left( \frac{1.7372 \times 10^{19} \text{ sec}}{t_0} \right) g_{*s}^{2/3} g_*^{-1/2} (1+z_i)^{-6} \Phi(E_i, z_i) \left( \frac{dE_i}{dE_0} \right)_{E_0}, & \text{if } z_i > z_{eq}. \end{cases}$$

In the above equations  $z_i$  is the redshift corresponding to the injection time  $t_i$ ,  $z_{eq}$  is the redshift of equal matter and radiation energy densities,  $t_0$  is the present age of the universe,  $E_0$  is the energy of the particles in the present epoch,  $E_i \equiv E_i(E_0, z_i)$  is the injection energy,  $z_{i,max}(E_0)$  is the maximum possible injection redshift corresponding to the earliest possible injection time  $t_{i,min}(E_0)$  for a given  $E_0$ , and  $g_{*s}$  and  $g_*$  are the total number of effective relativistic degrees of freedom contributing respectively to the entropy density and energy density of the universe[9] at the epoch  $z_i$ . The upper limit on  $z_{i,max}$  is given by  $E_i(E_0, z_{i,max}(E_0)) = m_x/2$ .

The energy-loss processes for UHE protons propagating through the cosmic medium, including the important Greisen-Zatsepin-Kuz'min (GZK)[10]-effect— whereby UHE protons above a certain threshold energy ( $\sim 5 \times 10^{10} \text{ GeV}$ ) catastrophically lose energy due to photopion production off the cosmic background photons— have been studied by many authors; for comprehensive discussions see, for example, Refs. [11,12]. For UHE protons we obtain the function  $E_i(E_0, z_i)$  by numerically solving the differential equation for energy

loss discussed in Ref. [12]. We find that for UHE protons  $z_{i,max} < 1.25$  at all energies of our interest.

For UHE neutrinos the relevant process is the absorption[13] of neutrinos through the process  $\nu + \bar{\nu}_{bb} \rightarrow \ell^+ \ell^-$ , where  $\ell = e, \mu, \tau, u, d, s, c$ , etc., and  $\bar{\nu}_{bb}$  represents the thermal background neutrinos (present temperature  $1.9^\circ K$ ). Denoting by  $z_a(E_{\nu,0})$  the redshift above which neutrinos of present energy  $E_{\nu,0}$  are absorbed due to the process mentioned above, we get

$$1 + z_a(E_{\nu,0}) = \begin{cases} 8.8143 \times 10^5 \left( \frac{GeV}{E_{\nu,0}} \right)^{1/3}, & \text{for } E_{\nu,0} < 3.08 \times 10^5 GeV, \\ 4.8286 \times 10^5 \left( \frac{GeV}{E_{\nu,0}} \right)^{2/7}, & \text{for } E_{\nu,0} \geq 3.08 \times 10^5 GeV. \end{cases}$$

Finally, for neutrinos, we have

$$1 + z_{i,max}(E_{\nu,0}) = \min \left( 1 + z_a(E_{\nu,0}), \frac{0.2134 m_x}{E_{\nu,0}} \right),$$

where we have used the fact[14] that the maximum neutrino energy is 0.4268 times the maximum pion energy ( $\sim m_x/2$ ).

The proton and neutrino differential spectra obtained by taking into account the energy loss of protons and absorption of neutrinos are shown in Figures 1 and 2 respectively for  $m_x = 10^{15} GeV$ . For any given value of  $p$  (see Eq. 1) we obtain an upper limit ( $\kappa_{max}$ ) on the ‘amplitude’  $\kappa$  for the process by requiring that the calculated UHE proton flux at any energy not exceed the observed UHE CR flux[15]; the results shown are for  $\kappa = \kappa_{max}$ . The evolved proton spectrum due to a proton injection spectrum  $\propto (1 + z_i)^{9/2} E_i^{-2.5}$  (hereafter called the “test spectrum”), continued to the energy  $m_x/2$ , is also shown in Fig. 1 for comparison. (Note that the index 9/2 of the redshift factor corresponds to the case of  $p = 1$  in Eq. 1). Comparison of the short-dashed curves (the ‘redshifted’ injection spectra) with the solid curves in Fig. 1 shows the effect of ‘photopion energy loss’ (the GZK-effect) on the UHE proton flux— the so-called “pile up” or “bump”[11,12] at  $E_0 \sim 5 \times 10^{10} GeV$  is clearly visible. Contrary to usual assumption, however, there is really *no complete* GZK-‘cutoff’ of the UHE proton spectrum associated with the photopion energy loss; instead  $E_0^3 j(E_0)$

only takes a “dip” after the “pile up” and then rises again as  $E_0$  increases further until it turns over before the final cutoff at  $E_0 \sim m_x/2$ . The spectrum flattening (‘recovery’) at  $E_0 \sim 1.8 \times 10^{11} GeV$  after the GZK-‘cutoff’ at  $E_0 \sim 5 \times 10^{10} GeV$  is partly due to a progressive decrease (with increasing energy) of the slope of the ‘photopion energy loss’ curve[12] for protons beginning at  $E_0 \sim 10^{11} GeV$ , and, of course, due to continuation of the injection spectrum to a much higher energy. Note that the recovery of the test spectrum (which, properly normalized, reproduces the observed UHE CR spectrum reasonably well at the observed energies; see Fig. 1), is much weaker because of its steeper injection spectrum.

The protons surviving at energies above the GZK-‘cutoff’ originate at small injection redshifts, and so the effect of source evolution (specified by the value of  $p$ ) on the final *shape* of the proton spectrum at these energies is small compared to that due to photopion energy loss. This, and the fact that the shape (though not the overall normalization) of the injection spectrum is determined by the physics of hadronic jet fragmentation independently of the value of  $p$ , lead to a universal (independent of the value of  $p$ ) spectrum *shape* for protons at these energies. The shape of the UHE neutrino spectrum, on the other hand, reflects the effect of source evolution (i.e., dependence on  $p$ ) because of higher possible injection redshifts.

For neutrinos we see from Fig. 2 that the lowest energy above which neutrinos from topological defects may be ‘visible’ above the atmospheric neutrino background[16] is smaller for processes with smaller values of  $p$ .

From Fig.1 it seems unlikely that topological-defect-induced UHE particles give any significant contribution to the observed UHE CR flux at energies below  $\sim 5 \times 10^{10} GeV$ . Above this energy, however, the topological defects can in principle give significant contribution to any (observed?[17]) CR flux. So, detection of UHE CR events at  $E_0 \gg 5 \times 10^{10} GeV$  may give us a signature of GUT in general and topological defects in particular. From Fig. 1 a rough power-law *approximation* to our universal UHE proton spectrum above

the GZK-‘cutoff’ gives  $j(E_0) \propto E_0^{-3.8}$  for  $4.5 \times 10^{10} GeV \leq E_0 < 1.8 \times 10^{11} GeV$  and  $j(E_0) \propto E_0^{-1.83}$  for  $1.8 \times 10^{11} GeV \leq E_0 \leq 5 \times 10^{13} GeV$ .

The maximal expected *integral* flux for both protons and neutrinos are shown in Fig. 3. The maximal proton integral flux above  $7 \times 10^{10} GeV$ , for example, is  $\sim 5 \times 10^{-16} m^{-2}.s^{-1}.sr^{-1}$  giving an event rate of  $\sim 5 \times 10^{-2} yr^{-1}.Km^{-2}$  in a  $\pi$  steradian detector. The numbers for neutrinos depend on the value of  $p$  and can be read off from Fig. 3. Thus for processes with values of  $\kappa$  not too small compared to the maximal values obtained above, the resulting UHE proton flux may be detectable in some of the planned large Extended Air Shower Arrays such as[18] the  $100Km^2$  AGASA experiment in Akeno, Japan, the “HiRes” detectors of the Fly’s Eye experiment, and the proposed  $1000Km^2$  array in USSR. Similarly the UHE neutrinos from these processes may be detectable in experiments like DUMAND[19].

To summarize, characteristic features of topological defect-induced hadronic CR spectrum include: (1) A spectrum flattening (‘recovery’) at  $\sim 1.8 \times 10^{11} GeV$  after the GZK steepening (‘cutoff’) at  $\sim 5 \times 10^{10} GeV$ , and continuation of the spectrum to a GUT scale energy with a *universal shape*; (2) hadronic component consists of protons and perhaps some neutrons, but *no* “heavies” such as *Fe* nuclei; and (3) presence of antiparticles in the primary spectrum, which may however be difficult to distinguish from particles at the extremely high energies we are considering.

Finally, the numerical results given above are for a specific value of  $m_x = 10^{15} GeV$ . The flux of particles at any given energy will be higher for a smaller value of  $m_x$ , but then the final cutoff of the spectrum shifts to a smaller value such that overall energy conservation is maintained.

PB is supported by NSF grant INT 91-10117 to the University of Chicago, CTH by DoE at Fermilab, and DNS in part by NSF grant AST 91-22629, by DoE grant DE-FG02-91 ER 40606 and by NASA grant NAGW 1321 at University of Chicago and by the DoE and NASA grant NAGW 1340 at Fermilab.

## References

- [1] For a review, see A. Vilenkin, *Phys. Rep.* **121**, 263 (1985).
- [2] C. T. Hill, *Nucl. Phys.* **B224**, 469 (1983).
- [3] C. T. Hill, D. N. Schramm and T. P. Walker, *Phys. Rev.* **D36**, 1007 (1987).
- [4] P. Bhattacharjee and N. C. Rana, *Phys. Lett.* **B246**, 365 (1990).
- [5] See P. Bhattacharjee, in Ref. [6], p. 382–399.
- [6] M. Nagano and F. Takahara (editors), *Astrophysical Aspects of the Most Energetic Cosmic Rays* (World Scientific, Singapore, 1991).
- [7] P. Bhattacharjee (in preparation).
- [8] See, for example, F. W. Stecker, *Astrophys. J.* **228**, 919 (1979).
- [9] E. W. Kolb and M. S. Turner, *The Early Universe* (Addison-Wesley, New York, 1990).
- [10] K. Greisen, *Phys. Rev. Lett.* **16**, 748 (1966); G. T. Zatsepin and V. A. Kuz'min, *JETP Lett.* **4**, 78 (1966).
- [11] C. T. Hill and D. N. Schramm, *Phys. Rev.* **D31**, 564 (1985).
- [12] V. S. Berezinsky and S. I. Grigor'eva, *Astron. Astrophys.* **199**, 1 (1988).
- [13] V. S. Berezinskii, S. V. Bulanov, V. A. Dogiel, V. L. Ginzburg, and V. S. Ptuskin, *Astrophysics of Cosmic Rays* (North Holland, 1990), Chapter VIII, p.354; V. S. Berezinsky, Bartol Preprint BA-90-87 (1990).
- [14] F. W. Stecker, *Cosmic Gamma Rays* (Mono Book Corp., Baltimore, 1971), p. 14–17.
- [15] R. M. Baltrusaitis et al., *Phys. Rev. Lett.* **54**, 1875 (1985) (Fly's Eye group).
- [16] K. Mitsui, Y. Minorikawa, and H. Komori, *Nuovo Cim.* **9 C**, 995 (1986).
- [17] M. A. Lawrence, R. J. O. Reid and A. A. Watson, *J. Phys. G.* **17**, 733 (1991).
- [18] See the articles by M. Nagano et al, E. C. Loh et al, and G. B. Khristiansen et al, respectively, in Ref. [6], p. 335–365.
- [19] See, for example, A. Okada (for DUMAND) in Ref.[6], p.483–486.
- [20] See P. Sokolsky, *Introduction to Ultrahigh Energy Cosmic Ray Physics* (Addison-Wesley, New York, 1989), p. 163.

## Figure Captions:

Fig. 1. The UHE proton spectrum due to topological defects. The four solid curves (which are indistinguishable for  $E_0 > 5 \times 10^{10} GeV$ ) are the maximal flux spectra for four different values of  $p$ . These correspond, from the lower-most solid curve to the uppermost solid curve, to  $p = 1.5, 1, 0.5$  and  $0$ , respectively, the corresponding values of  $\kappa_{max}$  being  $1.18 \times 10^{-29}$ ,  $0.2313$ ,  $4.52 \times 10^{27}$  and  $8.82 \times 10^{55}$ , respectively. The four short-dashed curves (“redshifted injection spectra”) correspond to the same four values and order of  $p$  and corresponding  $\kappa_{max}$  as above, but now calculated with no other energy loss of protons *except* that due to expansion of the universe. The dashed curve (terminating at  $7 \times 10^{10} GeV$ ) represents the UHE CR flux given by the Fly’s Eye group[15], and the dash-dotted curve immediately above it is for the “test spectrum” (see text). The normalization of the last curve has been conveniently chosen for clarity of display.

Fig. 2. The UHE neutrino spectra. The solid curves represent the maximal  $\nu_\mu + \bar{\nu}_\mu$  flux for the same set of values and order of  $p$  and corresponding  $\kappa_{max}$  as in Fig. 1.. The dashed curve represents the estimated horizontal atmospheric neutrino flux[16].

Fig. 3. The maximal *integral* UHE proton ( $p$ ) and neutrino ( $\nu$ ) spectra for the same values and order of  $p$  and corresponding  $\kappa_{max}$  as in Figs. 1 and 2. The dashed curve represents the UHE CR flux given by Fly’s Eye group[15] and the dash-dotted curve immediately above it is for the “test spectrum” with the same normalization as in Fig. 1. The two short-dashed curves marked  $\nu D$  and  $\nu U$  represent the *upper limits* on downward-going and upward-going neutrinos, respectively, given by the Fly’s Eye Group[20].

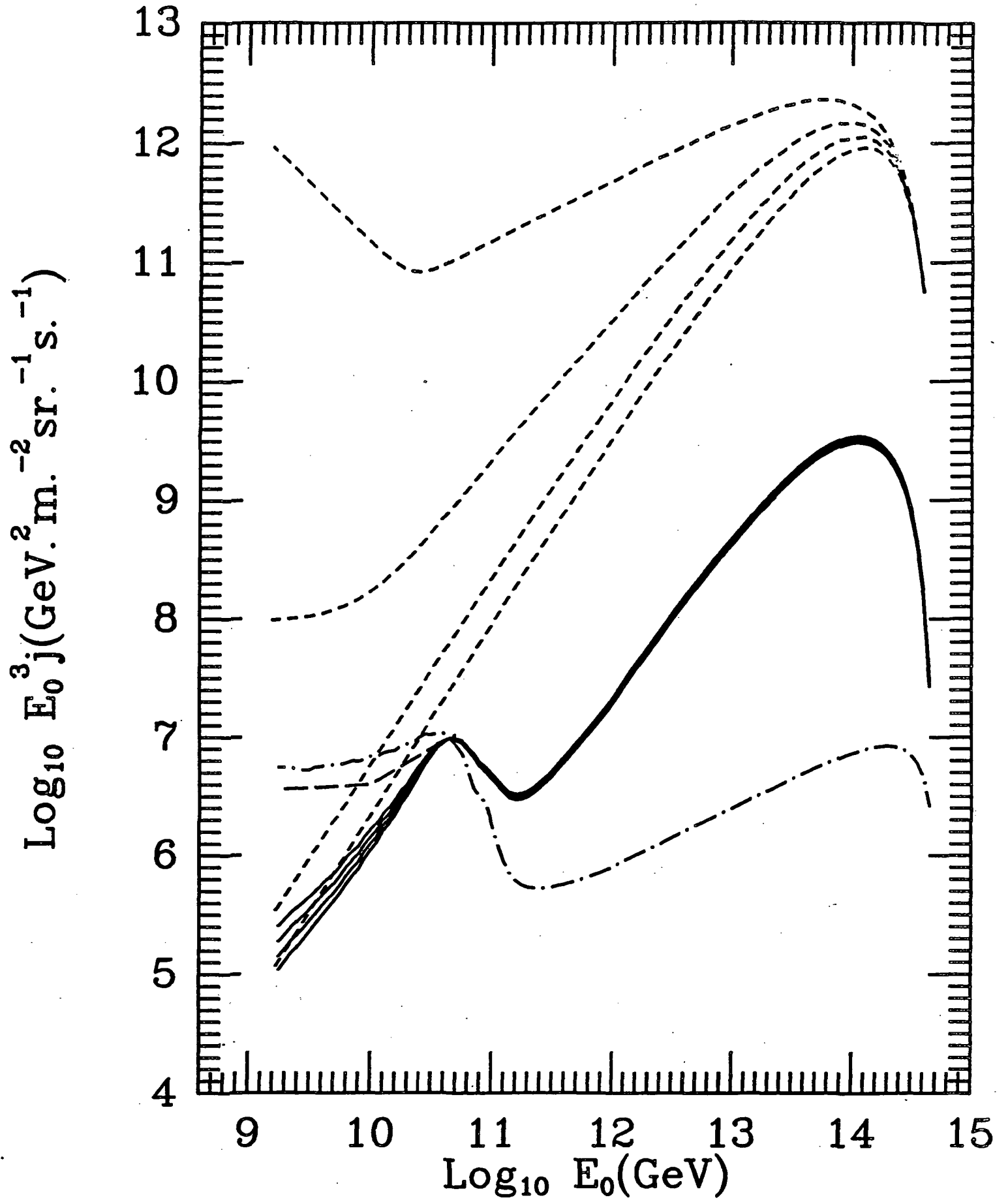


FIG. 1

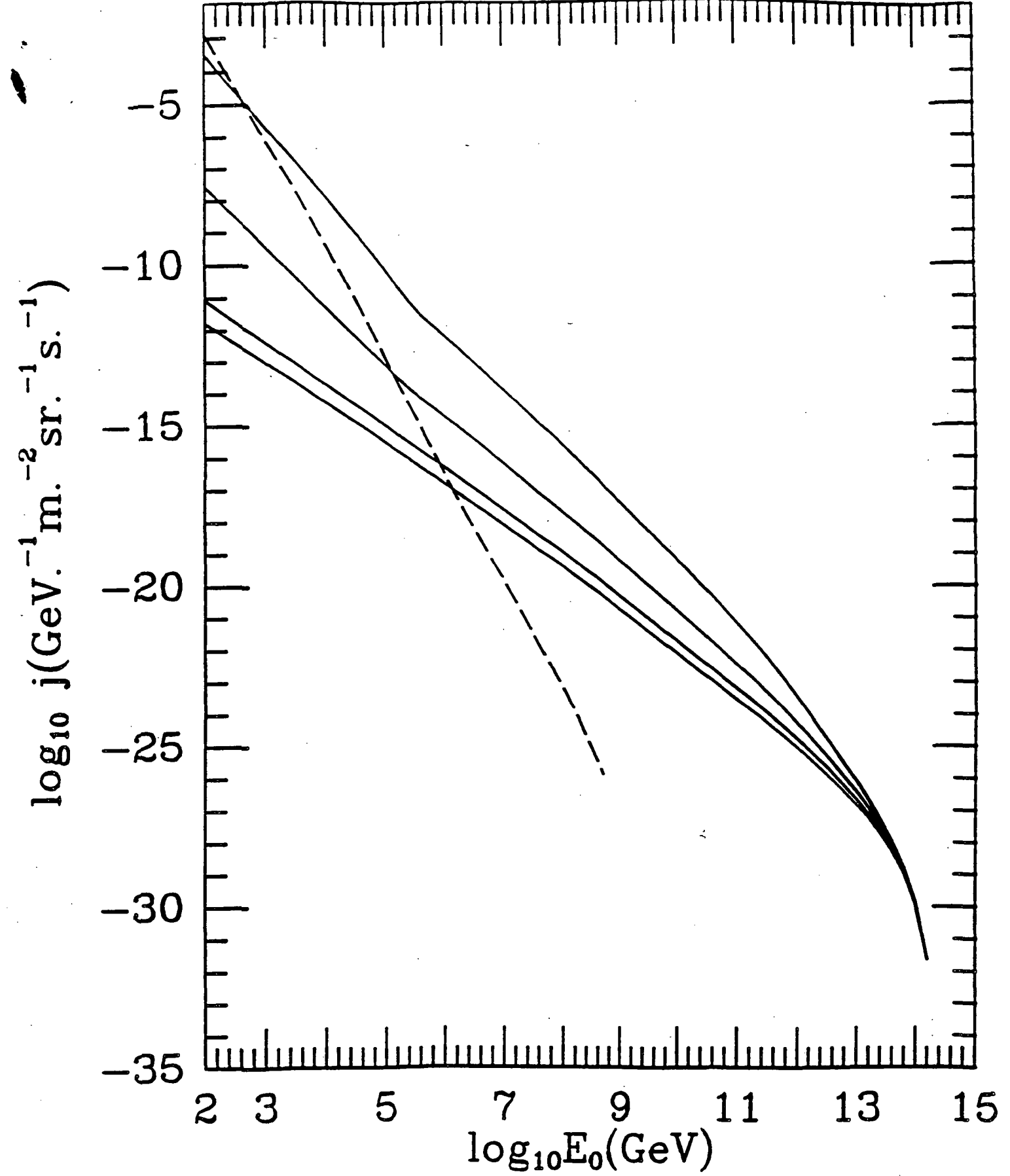


FIG. 2.

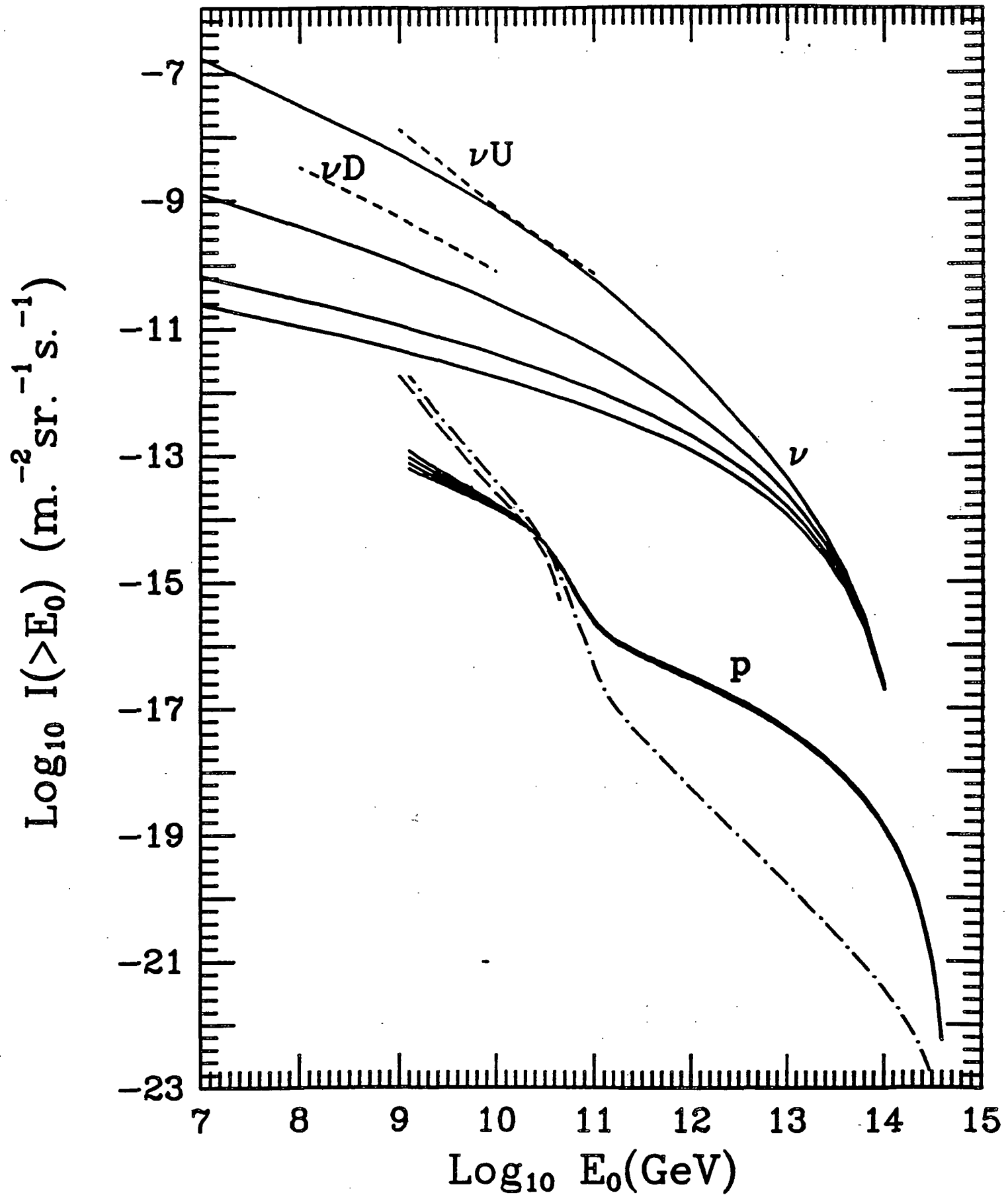


FIG. 3